

Research Article

Analysis of Vibration and Acoustic Characteristics of a Simply Supported Double-Panel Partition under Thermal Environment

Lei Guo ¹, Jianmin Ge ¹ and Shu Liu ²

¹College of Physical Science and Engineering, Tongji University, Shanghai 200092, China

²Appraisal Center for Environment & Engineering, Ministry of Environmental Protection, Beijing 100012, China

Correspondence should be addressed to Jianmin Ge; 1510551@tongji.edu.cn

Received 27 November 2019; Revised 6 January 2020; Accepted 22 January 2020; Published 25 February 2020

Academic Editor: Angelo Marcelo Tuset

Copyright © 2020 Lei Guo et al. This is an open access article distributed under the Creative Commons Attribution License, which permits unrestricted use, distribution, and reproduction in any medium, provided the original work is properly cited.

Numerical studies on the vibration and acoustic characteristics of a simply supported double-panel partition under the thermal environment are presented by the modal superposition approach and temperature field theory. Many factors are considered in this theoretical research, including acoustic refraction, dynamic response of the panel under thermal and acoustic load, vibroacoustic coupling characteristic analysis, and the variation of material properties. To access the accuracy and feasibility of the theoretical model, a finite element method is proposed to calculate the natural frequencies and mode shapes. The results show that the vibration and acoustic responses change obviously with the change of thermal stress and material properties. The rise of the graded thermal environment and thermal load decreases the natural frequencies and moves response peaks to the low-frequency range. The first valley of sound transmission loss is well consistent with the mode frequency. Finally, the relation between the average sound insulation and the thickness ratio is analyzed.

1. Introduction

Double-panel partition structure has been widely used in high-speed trains, aeronautics, and astronautics, due to its high strength, high stiffness-and-weight ratio, and good thermal and sound insulation performance [1]. High-speed trains and aircrafts are usually exposed to the external low-temperature condition or high-temperature environment caused by aerodynamic heating. The change of the thermal environment has a series of effects on the parameters of materials, the form of structure, and the state of stress [2–5]. Therefore, the study of vibration and acoustic characteristics of the double-panel partition under the thermal environment is of great significance for optimizing structural design, reducing interior noise, and improving transportation safety.

The mechanical and acoustic properties of elastic structures in the thermal environment have been studied by experiments, theories, and simulations. The thermal environment has lots of effects on the structure, including temperature-related material properties, thermal deformation, and thermal stress [6–8]. The

study of the relationship between temperature and acoustic material parameters begins with the phenomenon of sound velocity variation. Wayne carried out a research on the speed of sound and obtained the relationship between sound velocity and temperature under different pressures through a large number of experiments [9]. Kenneth studied the variation of density, thermal coefficient of thermal expansion, and thermal conductivity of common industrial alloy materials with temperature [10]. Li and He established a new aerodynamic heating method to conduct experiments and simulation studies on structural modal analysis under different temperature and temperature gradients [8]. Kehoe and Vivian [11] showed the change of material properties and the thermal stress is the main reason for the lower stiffness. Geng et al. [12] experimentally investigated the dynamic and acoustic response characteristics of a clamped rectangular aluminum plate under the thermal environment and analyzed the influence of the thermal environment on natural frequency through the modal test. With the increase of structure temperature, the natural frequency of the plate decreases obviously. The exchange of mode shape was observed at positions where the mode frequencies were close to

each other. In terms of theory, in 1935, Maulbetsch [13] studied the thermal stress problem of rectangular plates with simply supported conditions. By dividing the stress into internal stress and boundary force, the thermal stress in non-uniformly heated plates was calculated. Brischetto and Carrera [14] proposed a fully coupled thermal-mechanical method to obtain the mode count and modal density of single and double metal plates. Das and Navaratna [15] studied the bending and thermal stress of rectangular plates in the temperature gradient environment and focused on the influence of boundary conditions on the vibration equations. Liu and Li [16] obtained the natural frequency, mode shape, and dynamic response of the structure based on equivalent nonclassical theory and considering the influence of shear deformation and moment of inertia. Tauchert [17] systematically summarized the response of plate under thermal load, especially in thermal deformation, thermal buckling, and vibration characteristics. The influence of plate thickness, the form of plane, supporting conditions, and material characteristics on the thermoelastic design is theoretically analyzed. It is pointed out that the computational science based on the finite element method (FEM) and boundary element method (BEM) is an important means for further study. Thornton et al. [18] used the FEM to analyze the thermal buckling characteristics of thin plates induced by steady and unsteady spatial temperature gradients. Ganesan and Dhotarad [19] presented a study of vibration analysis of a thermally stressed plate. For the thermal stress analysis, the FEM was used, and for the vibration analysis, the finite difference method and calculus of variations were used. Qian et al. [20, 21] studied the dynamic response and radiation characteristics of a simply supported isotropic rectangular plate under the temperature gradient field by FEM/BEM simulations. Jeyaraj et al. [22–24] analyzed the vibration and sound radiation problems using a coupled FEM/BEM technique. The isotropic plates, composite plates with inherent material damping, and multilayered viscoelastic sandwich plates in a thermal environment were studied, respectively. Zhou et al. [25] proposed a closed-form solution to evaluate the free vibration of the orthotropic plate under the thermal environment, and the mode shapes obtained by the theoretical solution are well consistent with FEM results.

The objective of this work is to obtain a theoretical model for the vibroacoustic characteristics of a simply supported double-panel partition under the thermal environment. The temperature inside the structure is assumed to change evenly along the thickness direction. The formulation is derived by using the modal superposition approach and temperature field theory. Many factors are also considered in this theoretical research, including acoustic refraction, dynamic response of the panel under thermal and acoustic load, vibroacoustic coupling characteristic analysis, and the variation of material properties. The accuracy and validity of the theoretical predictions are checked against FEM results. Finally, the parametric study focusing on the influence of the temperature gradient and shape parameter on the vibroacoustic characteristics of a simply supported double-panel partition is deeply discussed.

2. Theoretical Formulation

Here, we consider a simply supported double-panel partition with dimensions of $a \times b \times (h_1 + H + h_2)$, in which the thickness of the bottom panel is h_1 , the thickness of the top panel is h_2 , and the thickness of the cavity is H , as shown in Figure 1. The double-panel partition divides the spatial space into three fields, i.e., sound incident field, sound cavity field, and sound radiating field. An incident plane sound wave impinges on the bottom panel with the elevation angle φ and the azimuth angle θ . The vibration of the incident panel caused by the excitation of the incident sound wave influences the radiant panel through the sound cavity field and radiates the sound waves into the radiating field. In this paper, it is assumed that the panel has no thermal stress at the reference temperature T_0 , and the temperature inside the structure changes evenly along the thickness direction under the thermal environment.

2.1. Bending of Sound Wave Paths under Thermal Environment. According to the wave equation, motion equation, and gas state equation of sound propagation [26], the relationship between sound velocity and temperature is deduced as

$$c = \sqrt{\frac{\gamma P}{\rho}} \sqrt{T}, \quad (1)$$

where c is the sound velocity, γ is the specific heat ratio, P is the pressure, ρ is the density, and T is the temperature. When the influence of gas components on the sound velocity is ignored, the acoustic propagation velocity can be regarded as a single-valued function of the absolute temperature of the gas medium. Since the temperature in the cavity varies uniformly with the direction of thickness, the sound velocity c is only related to the coordinate z , which is denoted as $c = c(z)$. Considering the sound wave is located in the x - z plane, the sound velocity gradient in the x direction is zero. The relations between sound velocity and propagation path can be written as [27]

$$\frac{d}{ds} \left(\frac{c_0}{c} \cos \alpha \right) = 0, \quad (2)$$

$$\frac{d}{ds} \left(\frac{c_0}{c} \cos \varphi \right) = -\frac{c_0}{c^2} \frac{dc}{dz}, \quad (3)$$

where s is the propagation path of the sound wave and α is the angle between the incident sound wave and the x axis, defined as $\alpha = \pi/2 - \varphi$. When the initial values of c_0 and α_0 are given, the ratio of $\cos \alpha$ to $c(z)$ remains constant along the sound propagation path [28], expressed as

$$\frac{\cos \alpha}{c(z)} = \frac{\cos \alpha_0}{c_0}. \quad (4)$$

Then, equations (2)–(4) can be simplified into

$$\frac{d\varphi}{ds} = \frac{\sin \varphi}{c} \frac{dc}{dz}. \quad (5)$$

For the medium with a constant temperature gradient, the actual temperature can be expressed as

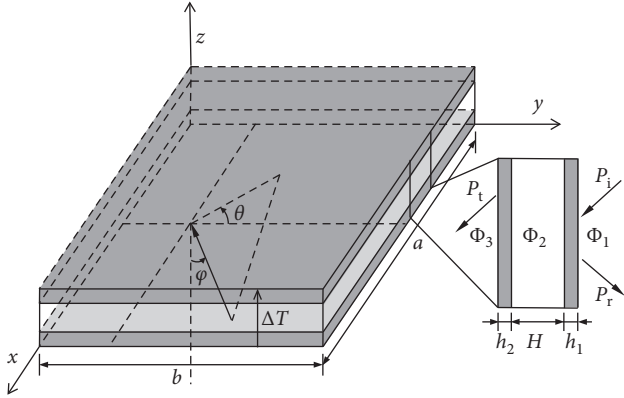


FIGURE 1: Schematic illustration of a simply supported double-panel partition under the thermal environment.

$$T = T_0 + kz, \quad (6)$$

where k is the temperature gradient ratio and is considered a constant. Substituting equation (6) into equation (1), the relations between sound velocity and z can be written as

$$c = c_0 \sqrt{1 + \frac{kz}{T_0}}, \quad (7)$$

$$\frac{dc}{dz} = \frac{kc_0}{2\sqrt{T_0^2 + kT_0z}}. \quad (8)$$

It can be deduced from equations (5)–(8) that the curvature of the sound wave varies with the propagation path under the constant temperature gradient environment. When the sound velocity gradient is negative, the sound waves bend in the direction of the temperature reduction. Therefore, one of the important functions of the thermal environment is to induce the refraction effect of sound waves. The refraction effect on incident sound waves at different incident angles is different.

2.2. Thermal Stress Analysis. It is assumed that the panel has no thermal stress at the reference temperature T_0 . When the temperature changes to T , the thermal stress will change the stress state of the structure. As the temperature inside the structure changes evenly along the thickness direction, the thermoelastic parameter can be described by the plane stress state, expressed as follows [29]:

$$\begin{aligned} \sigma_x &= \sigma_x(x, y), \\ \sigma_y &= \sigma_y(x, y), \\ \tau_{xy} &= \tau_{xy}(x, y), \\ \sigma_z &= \tau_{xz} = \tau_{yz} = 0. \end{aligned} \quad (9)$$

Under the thermal environment, the stress-displacement relations can be expressed as

$$\sigma_x = \frac{E}{1-\nu^2} [(\varepsilon_x + \nu\varepsilon_y) - \alpha(1+\nu)(T-T_0)], \quad (10)$$

$$\sigma_y = \frac{E}{1-\nu^2} [(\varepsilon_y + \nu\varepsilon_x) - \alpha(1+\nu)(T-T_0)], \quad (11)$$

$$\tau_{xy} = \frac{E}{1+\nu}\varepsilon_{xy}, \quad (12)$$

where E is Young's modulus, ν is Poisson's ratio, and α is the thermal expansion coefficient of the panel. No in-plane displacement will be caused as the double-panel partition is simply supported. Then, equations (10)–(12) can be simplified into

$$\sigma_x = -\frac{E\alpha\Delta T}{1-\nu}, \quad (13)$$

$$\sigma_y = -\frac{E\alpha\Delta T}{1-\nu}, \quad (14)$$

$$\tau_{xy} = 0, \quad (15)$$

where $\Delta T = T - T_0$ is denoted as the temperature change. The thermal stress of the panel can be obtained by integrating equations (13)–(15) in the direction of thickness, expressed as follows:

$$\begin{cases} N_{ix} \\ N_{iy} \\ N_{ixy} \end{cases} = \int_{-(h_i/2)}^{+(h_i/2)} \begin{cases} \sigma_x \\ \sigma_y \\ \tau_{xy} \end{cases} dz = \begin{cases} \frac{\alpha E \Delta T h_i}{1-\nu} \\ \frac{\alpha E \Delta T h_i}{1-\nu} \\ 0 \end{cases}, \quad i = 1, 2. \quad (16)$$

2.3. Coupling Theory for Simply Supported Double-Panel Partition under Thermal Environment. Due to the excitation of the incident sound wave, the vibroacoustic coupling equation of the simple supported double-panel partition under the thermal environment can be expressed as

$$D_1 \nabla^4 w_1 + m_1 \frac{\partial^2 w_1}{\partial t^2} - N_x \frac{\partial^2 w_1}{\partial x^2} - N_y \frac{\partial^2 w_1}{\partial y^2} - (p_1 - p_2) = 0, \quad (17)$$

$$D_2 \nabla^4 w_2 + m_2 \frac{\partial^2 w_2}{\partial t^2} - N_x \frac{\partial^2 w_2}{\partial x^2} - N_y \frac{\partial^2 w_2}{\partial y^2} - (p_2 - p_3) = 0, \quad (18)$$

where (w_1, w_2) , (m_1, m_2) , and (D_1, D_2) are transverse displacement, areal density, and flexural rigidity of the panels, respectively; subscripts 1 and 2 represent the bottom and top panels; and (p_1, p_2, p_3) is the sound pressure in the sound incident field, sound cavity field, and sound radiating field. The flexural rigidity is defined as

$$D_i = \frac{E_i h_i^3 (1 + j\eta_i)}{12(1 - \nu_i^2)}, \quad i = 1, 2, \quad (19)$$

where η is the material loss factor. As the double-panel partition is simply supported, the transverse displacement and bending moment at the boundary of the panel ($x=0, a$; $y=0, b$) are zero. The simply supported boundary conditions can be mathematically described as

$$\begin{aligned} w_i &= 0, \\ \frac{\partial^2 w_i}{\partial x^2} = \frac{\partial^2 w_i}{\partial y^2} &= 0, \end{aligned} \quad (20)$$

$$i = 1, 2.$$

For a simply supported double-panel partition system excited by a harmonic sound wave, the transverse placement of the panel can be written as

$$w_i(x, y, t) = \sum_{m=1}^{\infty} \sum_{n=1}^{\infty} \phi_{mn}(x, y) q_{i,mn}(t), \quad i = 1, 2, \quad (21)$$

where ϕ_{mn} is the modal shape function and $q_{i,mn}$ is the modal displacement coefficients, expressed as

$$\phi_{mn}(x, y) = \sin \frac{m\pi x}{a} \sin \frac{n\pi y}{b}, \quad (22)$$

$$q_{i,mn}(t) = \alpha_{i,mn} e^{j\omega t}, \quad i = 1, 2,$$

where $\alpha_{i,mn}$ is modal coefficients. The sound pressure distribution in the air space of the double-panel partition should have the same series form as the modal function. So, the velocity potentials in the sound incident field, sound cavity field, and sound radiating field near the panel can be written as

$$\Phi_1(x, y, z; t) = \sum_{m=1}^{\infty} \sum_{n=1}^{\infty} \left[I_{mn} \varphi_{mn}(x, y) e^{-j(k_{1z}z - \omega t)} + \beta_{mn} \varphi_{mn}(x, y) e^{-j(-k_{1z}z - \omega t)} \right], \quad (23)$$

$$\Phi_2(x, y, z; t) = \sum_{m=1}^{\infty} \sum_{n=1}^{\infty} \left[\varepsilon_{mn} \varphi_{mn}(x, y) e^{-j(k_{2z}z - \omega t)} + \zeta_{mn} \varphi_{mn}(x, y) e^{-j(-k_{2z}z - \omega t)} \right], \quad (24)$$

$$\Phi_3(x, y, z; t) = \sum_{m=1}^{\infty} \sum_{n=1}^{\infty} \xi_{mn} \varphi_{mn}(x, y) e^{-j(k_{3z}z - \omega t)}, \quad (25)$$

where $I, \beta, \varepsilon, \zeta,$ and ξ and can be obtained by

$$\begin{aligned} \tilde{\lambda}_{mn} &= \frac{4}{ab} \int_0^b \int_0^a \tilde{\lambda} e^{-j(k_x x + k_y y)} \sin \frac{m\pi x}{a} \sin \frac{n\pi y}{b} dx dy, \\ \tilde{\lambda} &= I, \beta, \varepsilon, \zeta, \xi. \end{aligned} \quad (26)$$

The sound pressure can be obtained by

$$p_i = \rho_i \frac{\partial \Phi_i}{\partial t} = j\omega \rho_i \Phi_i, \quad i = 1, 2, 3. \quad (27)$$

At the interface between the air and the panel, the velocity continuity condition can be expressed as

$$z = 0: \quad -\frac{\partial \Phi_1}{\partial z} = j\omega w_1, \quad -\frac{\partial \Phi_2}{\partial z} = j\omega w_1, \quad (28)$$

$$z = H: \quad -\frac{\partial \Phi_2}{\partial z} = j\omega w_2, \quad -\frac{\partial \Phi_3}{\partial z} = j\omega w_2. \quad (29)$$

Substituting equations (23)–(25) into equations (28) and (29) yields

$$\beta_{mn} = I_{mn} - \frac{\omega \alpha_{1,mn}}{k_{1z}}, \quad (30)$$

$$\varepsilon_{mn} - \zeta_{mn} = \frac{\omega \alpha_{2,mn}}{k_{2z}}, \quad (31)$$

$$\varepsilon_{mn} e^{-jk_{2z}H} - \zeta_{mn} e^{jk_{2z}H} = \frac{\omega \alpha_{2,mn}}{k'_{2z}H + k_{2z}(H)}, \quad (32)$$

$$\xi_{mn} = \frac{\omega \alpha_{2,mn} e^{jk_{3z}H}}{k_{3z}}. \quad (33)$$

Substituting equations (30)–(33) into equations (17) and (18) by using the virtual work principle, the equations can be simplified into [27]

$$\begin{aligned}
& \left\{ D_1 \varphi_0 - m_1 \omega^2 - \frac{\alpha E \Delta T h_1}{1 - \nu} \left[\left(\frac{m\pi}{a} \right)^2 + \left(\frac{n\pi}{b} \right)^2 \right] + j\omega \rho_1 \frac{\omega}{k_{1z}} - j\omega \rho_2 \frac{\omega (1 + e^{2jk_{2z,H}H})}{k_{2z,0} (1 - e^{2jk_{2z,H}H})} \right\} \alpha_{1,mn} \\
& + \left[j\omega \rho_2 \frac{2\omega e^{jk_{2z,H}H}}{(k'_{2z,H}H + k_{2z,H}) (1 - e^{2jk_{2z,H}H})} \right] \alpha_{2,mn} = 2j\omega \rho_1 I_{mn} \left[j\omega \rho_3 \frac{2\omega e^{jk_{2z,H}H}}{k_{2z,0} (1 - e^{2jk_{2z,H}H})} \right] \alpha_{1,mn} \quad (34) \\
& + \left\{ D_2 \varphi_0 - m_2 \omega^2 - \frac{\alpha E \Delta T h_2}{1 - \nu} \left[\left(\frac{m\pi}{a} \right)^2 + \left(\frac{n\pi}{b} \right)^2 \right] + j\omega \rho_4 \frac{\omega}{k_{3z}} - j\omega \rho_3 \frac{\omega (1 + e^{2jk_{2z,H}H})}{(k'_{2z,H}H + k_{2z,H}) (1 - e^{2jk_{2z,H}H})} \right\} \alpha_{2,mn} = 0.
\end{aligned}$$

It can be deduced from equation (33) that the natural frequency of the double-panel partition under the thermal environment is stated as

$$\omega_{mn} = \sqrt{\pi^4 \left(\frac{m^2}{a^2} + \frac{n^2}{b^2} \right)^2 \frac{D_0}{\rho_i h_i} - \frac{\alpha E \Delta T}{\rho_i (1 - \nu)} \left[\left(\frac{m\pi}{a} \right)^2 + \left(\frac{n\pi}{b} \right)^2 \right]} \quad (35)$$

The transmission coefficient of sound power is defined as

$$\tau(\varphi, \theta) = \frac{\sum_{m=1}^{\infty} \sum_{n=1}^{\infty} |\xi_{mn}|^2}{\sum_{m=1}^{\infty} \sum_{n=1}^{\infty} |I_{mn} + \beta_{mn}|^2}. \quad (36)$$

3. Numerical Results and Discussion

3.1. Validation and Vibration Analysis. The vibration and acoustic responses of a simply supported double-panel partition change obviously with the change of thermal stress and material properties under the thermal environment. The finite element method can be used to solve the mode frequencies and mode shapes based on prestress calculation, and the results can be compared and verified with the theoretical calculation results. As shown in Figure 1, a simply supported double-panel partition with dimensions of $330 \times 250 \text{ mm}^2$ is considered here. The thickness of the bottom and top panels is 2 mm, and the thickness of the cavity field is 80 mm. The panel material is aluminum alloy with loss factor 0.001. Other material properties change with temperature, including mass density, Young's modulus, coefficient of thermal expansion, and Poisson's ratio, which are shown in Table 1 [10, 30]. Because the thermal conductivity of the air layer is far less than that of the aluminum alloy material, in general the thermal insulation performance of the double-panel partition is mainly assumed by the intermediate air layer under the thermal environment. The internal temperature gradient of the aluminum alloy is relatively small, so the change of material properties in a single metal panel is not considered in theoretical calculation. The temperature gradients considered in this paper are all within the critical buckling temperature range.

The temperature of the bottom panel is fixed at 25°C , and the temperature of the top panel is changed in different

thermal conditions. The direction of the temperature gradient is from the high-temperature side to the low-temperature side. The temperature difference within the bottom panel, cavity, and top panel is denoted by ΔT_1 , ΔT_2 , and ΔT_3 . The natural frequency of the double-zpanel partition under the thermal environment can be calculated based on theoretical formulation. As the properties of the material change with temperature, single-value variation analysis is performed on different material properties, and the results are shown in Figure 2. The temperature gradient of two panels is maintained at 1°C , and the temperature of the thermal environment changes. Only one material property change is considered in each curve, and other properties of the material are taken as $T = 25^\circ\text{C}$. As can be seen from Figure 2, the density, Young's modulus, and thermal expansion coefficient of the panel have a greater effect on the change of the first-order natural frequency due to the influence of temperature, while Poisson's ratio has a relatively smaller effect. With the increase of temperature, the density decreases and the first-order natural frequency moves to the high-frequency region. Young's modulus decreases with the increase of temperature; as a result, the bending stiffness decreases and the first-order natural frequency moves to the low-frequency region. The influence of the coefficient of thermal expansion and Poisson's ratio is mainly reflected in the thermal stress term in equation (35). Poisson's ratio has the least influence on the overall mode frequency change. Therefore, when considering the vibration analysis of a simply supported structure affected by the temperature environment, the change of material properties must be considered.

Considering the simultaneous changes of various material properties with temperature, based on the theoretical formula, the change of the first-order mode frequency with temperature is shown in Figure 3. When the temperature gradient is fixed at 1°C , the first-order natural frequency of the panel gradually moves to the low-frequency region with the increase of temperature. The decreasing trend of frequency is basically the same at different temperature. As shown in Figures 2 and 3, the thermal expansion coefficient and Young's modulus have the greatest influence on the natural frequency of the panels.

To access the accuracy and feasibility of the theoretical model, a finite element method is proposed to calculate the natural frequencies and mode shapes. The temperature distribution and thermal stress of the double-panel partition

TABLE 1: Aluminum alloy material parameters with temperature variation.

Temperature (°C)	Density (kg/m ³)	Young's modulus (GPa)	Coefficient of thermal expansion ($\times 10^6$)	Poisson's ratio
25	2750	71.70	22.9	0.331
100	2737	71.18	23.6	0.333
200	2717	70.49	24.3	0.337
300	2693	69.91	25.0	0.332
400	2668	69.31	25.7	0.320
500	2646	68.70	26.4	0.308

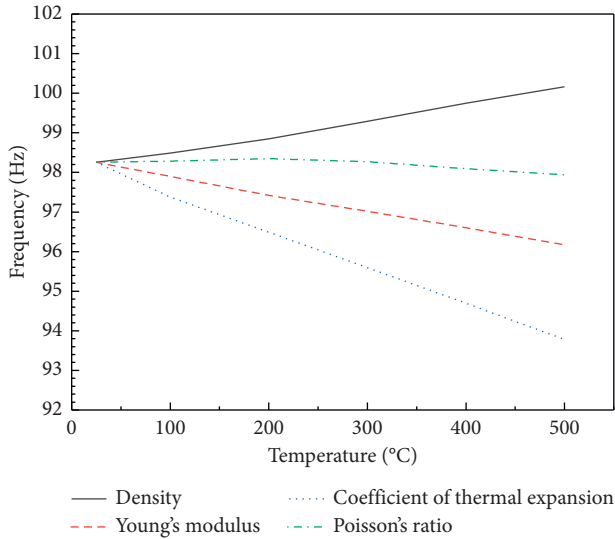


FIGURE 2: First-order natural frequency univariate analysis.

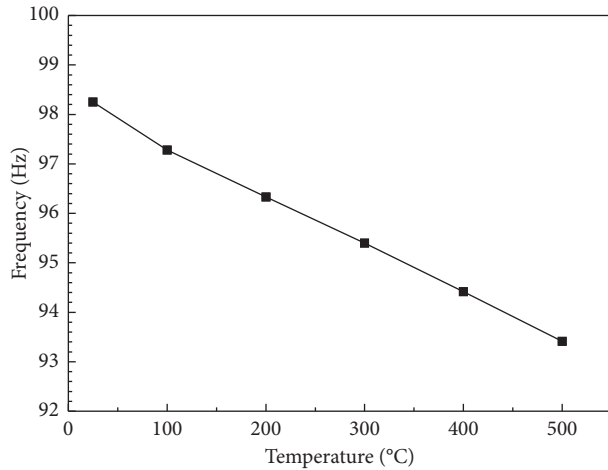


FIGURE 3: First-order natural frequency with temperature variation.

can be calculated by ANSYS software. The change of material properties with temperature is also considered in this simulation. The mode frequency variation of the double-panel partition under different temperature and temperature gradients is calculated. The first eight mode shapes and natural frequencies of the bottom panel are shown in Table 2, with the center temperature at 25°C and $\Delta T_1 = 1^\circ\text{C}$. The theoretical and predicted values of mode frequencies of the simply supported double-panel partition are in good

agreement. This indicates that the theoretical formula can well reflect the vibration characteristics of this structure.

Based on the theoretical model, the first eight orders of mode frequencies of the simply supported double-panel partition are calculated under the temperature gradient of 0~5°C in this paper, as shown in Table 3. As can be seen from Table 3, with the increase of the temperature gradient, the mode frequency of the same order moves to the low-frequency region. The first mode frequency and mode shape cannot be observed when the temperature gradient is greater than 3°C. But the change of the temperature gradient does not change the order of mode sequences and mode shapes.

3.2. Acoustic Analysis. The sound transmission loss of the double-panel partition is closely related to the incident angle, panel thickness, and cavity thickness at normal temperature [31]. It is also related to the temperature and temperature gradient under the thermal environment. The dimensions and material properties of the double-panel partition are the same as above. Figure 4 shows the sound transmission loss of the simply supported structure at different temperature gradients under the vertical incidence. Known from the results shown in Figure 4(a), the peak and trough of the vertically incident sound transmission loss curve of the simply supported double-panel partition move to the low-frequency region with the increase of the temperature gradient. Under the temperature gradient of 0°C, 1°C, and 2°C, the first trough of the vertically incident sound transmission loss of the simply supported double-panel partition is 123 Hz, 99 Hz, and 64 Hz, respectively, which are consistent with the first mode frequency in Table 3. Therefore, the first trough of the sound transmission loss curve is determined by the first-order vibration mode of the panel. Figure 4(b) expands the frequency calculation range to 10000 Hz on the basis of Figure 4(a). In the high-frequency region, the temperature gradient has little effect on the sound transmission loss under the vertical incidence. On the one hand, the deviation ratio of high mode frequency is relatively small. On the other hand, the transmission loss in high frequency is in the mass-controlled region and is determined by panel-cavity-panel dimensions and standing wave resonance. Under the same temperature gradient and different sound incidence angles, the acoustic transmission loss of the double-panel partition is calculated, and its variation trend is similar to that in Figure 4.

The temperature gradient in each panel is fixed at 2°C, and the thickness of the double-panel partition remains

TABLE 2: Comparisons of analytical and numerical results for the first-order natural frequency ($\Delta T_1 = 1^\circ\text{C}$).

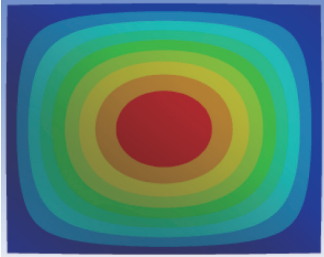
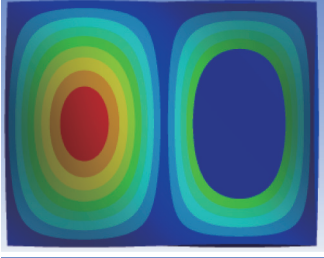
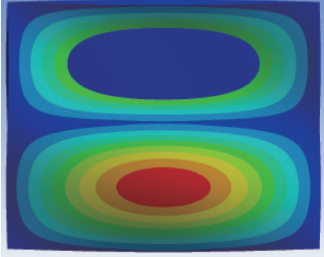
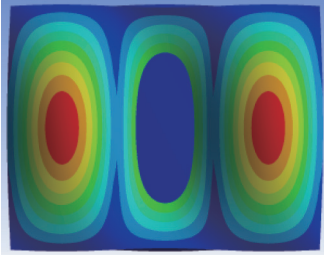
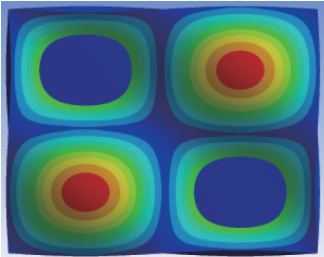
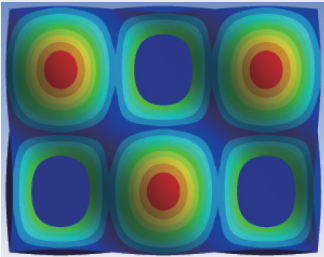
No.	Mode sequence	Mode shape	Numerical (Hz)	Analytical (Hz)	Error (%)
1	(1, 1)		98.3	96.5	-1.8
2	(2, 1)		234.9	230.8	-1.8
3	(1, 2)		335.6	340.4	1.4
4	(3, 1)		460.8	454.2	-1.4
5	(2, 2)		471.0	468.7	-0.5
6	(3, 2)		696.5	693.9	-0.4

TABLE 2: Continued.

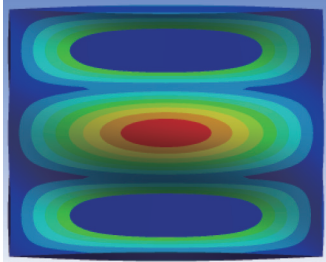
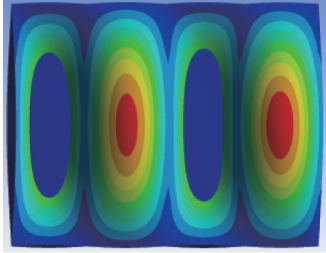
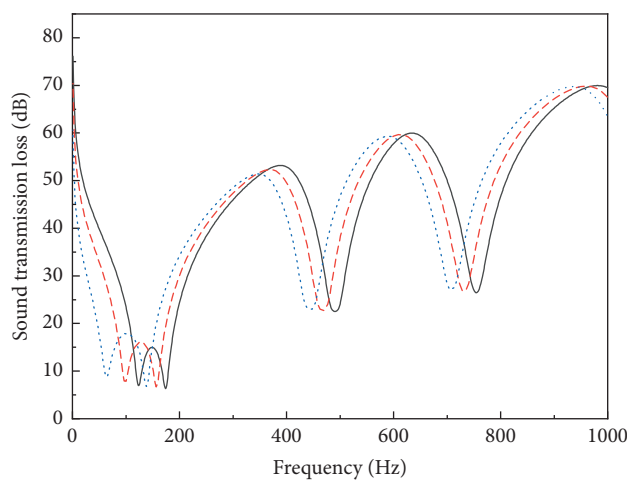
No.	Mode sequence	Mode shape	Numerical (Hz)	Analytical (Hz)	Error (%)
7	(1, 3)		728.6	740.2	1.6
8	(4, 1)		776.5	774.2	-0.3

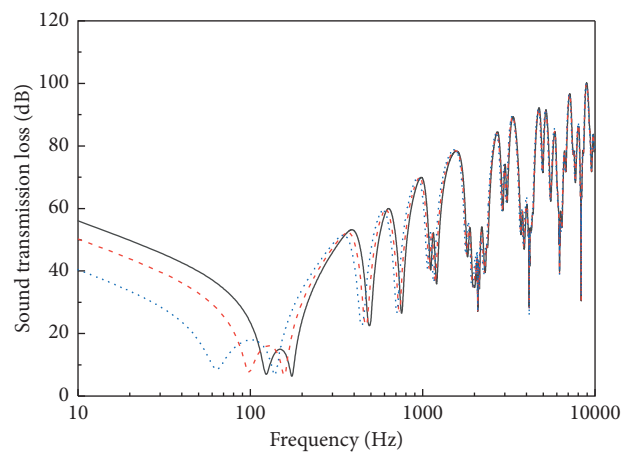
TABLE 3: Variation of natural frequencies with temperature.

Mode sequence	Temperature gradient (°C)					
	0	1	2	3	4	5
(1, 1)	123.6	98.3	63.5	—	—	—
(2, 1)	258.8	234.9	208.4	178.0	141.1	90.2
(1, 2)	359.1	335.6	310.4	282.8	252.3	217.6
(3, 1)	484.1	460.8	436.3	410.3	382.5	352.6
(2, 2)	494.3	471.0	446.6	420.6	393.0	363.3
(3, 2)	719.6	696.5	672.6	647.9	622.1	595.2
(1, 3)	751.7	728.6	704.8	680.1	654.5	627.9
(4, 1)	799.5	776.5	752.7	728.1	702.7	676.4



— Temperature gradient 0°C
 - - - Temperature gradient 1°C
 ····· Temperature gradient 2°C

(a)



— Temperature gradient 0°C
 - - - Temperature gradient 1°C
 ····· Temperature gradient 2°C

(b)

FIGURE 4: Sound transmission loss of a simply supported double-panel partition under different thermal environment. (a) Frequency region 0~1000 Hz. (b) Frequency region 0~10000 Hz.

constant. Scaling up the length and width of the panel, the vertically incident sound transmission loss is shown in Figure 5. As can be seen from Figure 5, when the size of the panel increases, the number of peaks and troughs on the curve decreases gradually and the curve becomes smoother. It shows that the small-size structure has more mode density than the large-size structure under the simply supported condition. In the middle- and high-frequency areas, with the increase of the size of the double-panel partition, the transmission loss curves tend to be overlapping. The vertically incident sound transmission loss curve of the infinite simply supported double-panel partition provides an upper limit reference for the acoustic transmission loss of finite ones.

The first trough of the vertically incident sound transmission loss of the simply supported double-panel partition tends to a fixed value as the panel size increases and corresponds to panel-cavity-panel resonance frequency, expressed as [32]

$$f_{\alpha} = \frac{1}{2\pi \cos \varphi} \sqrt{\frac{\rho c_0^2}{H} \frac{(m_1 + m_2)}{m_1 m_2}}. \quad (37)$$

The calculated result is 123.9 Hz, which is consistent with the position of the first sound transmission loss trough of the infinite panel in Figure 5. When the thickness of the cavity is an integral multiple of half wavelength of the incident sound wave, standing wave resonance will occur in the simply supported double-panel partition, which corresponds to the other sound transmission troughs of the infinite panels.

Based on equation (36), the influence of temperature on the sound transmission loss of the simply supported double-panel partition under the random-incidence sound field is calculated, as shown in Figure 6. The influence of the thermal environment on the sound transmission loss is mainly under 1000 Hz. With the increase of the temperature gradient, the sound transmission loss curve appears to cross in the low-frequency region. The natural frequencies move to the low-frequency region with the increase of the temperature gradient, which changes the acoustic performance of the double-panel partition. The sound transmission loss of the double-panel partition increases gradually with the increase of the temperature gradient in the 1/3 octave spectrum with the center frequency of 500 Hz. This indicates that the thermal stress caused by the temperature gradient causes the skewing and recombination of mode frequency in the damping-controlled region. Under the appropriate temperature gradient condition, the transmission loss at partial frequency can be increased.

The double-panel partition should maintain a certain working intensity and good thermal and sound insulation performance in the practical application. Considering that the thickness of the cavity and the total thickness of the bottom and top panels remain constant, this paper studies the variation of the transmission loss of the double-panel partition under the thermal environment and different thickness ratios of the panels. The thickness ratio of the panels is written as

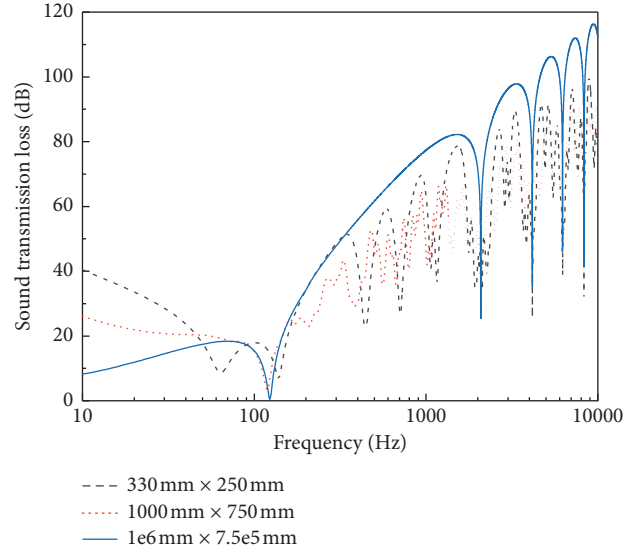


FIGURE 5: Influence of the size of the double-panel partition on the sound transmission loss in vertical incidence.

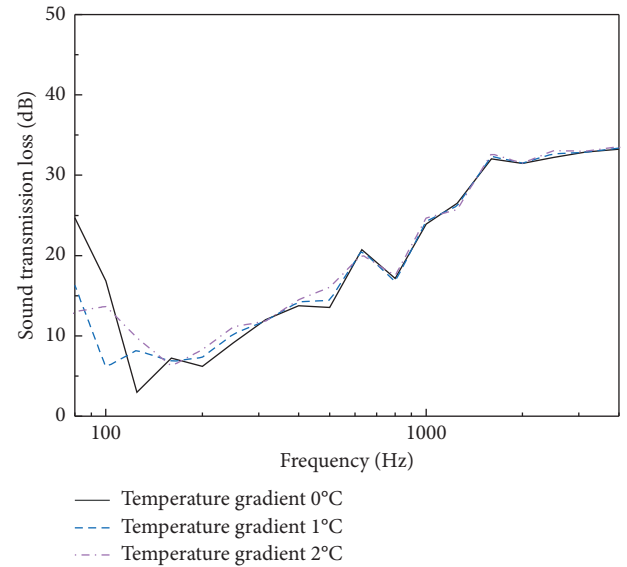


FIGURE 6: Influence of the temperature gradient on the sound insulation of a simply supported double-panel partition.

$$r = \frac{h_1}{h_2}. \quad (38)$$

The total thickness of the two panels is 4 mm, and the temperature gradient in each panel is fixed at 2°C. In order to maintain a good structural strength, the thickness ratio range is set at 0.1~10. For the convenience of comparison, the average sound transmission loss is selected as the evaluation index of the acoustic insulation performance of the double-panel partition, which can be expressed as

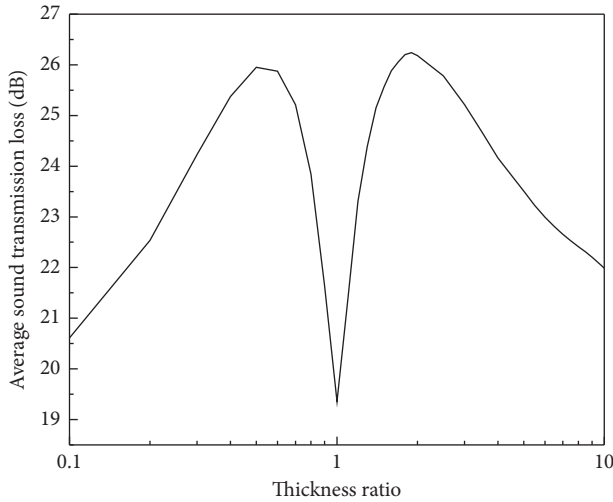


FIGURE 7: The average sound insulation of a simply supported double-panel partition under different thickness ratios.

$$R_{\text{ave}} = \frac{1}{n} \sum_{i=1}^n R_i, \quad (39)$$

where R_{ave} is the average sound transmission loss, R_i is the sound insulation at 1/3 octave band center frequencies from 100 Hz to 3150 Hz, and n is 16. The variation of the average sound transmission loss of the double-panel partition under different thickness ratios is shown in Figure 7. When the thickness ratio approaches 0.5 or 1.9, the average sound transmission loss of this structure is relatively larger. When the thickness ratio is close to 1, which means the thickness of the two panels is the same, the average sound transmission loss is significantly reduced. In addition, the average sound transmission loss reaches the maximum value when the thickness ratio is close to 1.9, which is 0.3 dB higher than that when the thickness ratio is 0.5. This indicates that the thickness ratio of the double-panel partition should be considered around 1.9 under the thermal environment and the thickness of the incident panel should be larger than that of the radiant panel.

4. Conclusions

In this paper, numerical studies on the vibration and acoustic characteristics of a simply supported double-panel partition under the thermal environment are presented based on the modal superposition approach and temperature field theory. The accuracy and feasibility of the theoretical model are verified by ANSYS FEM. Some conclusions are drawn as follows:

- (1) Under the same temperature gradient, the thermal expansion coefficient and Young's modulus have a greater influence on the natural frequency of the panels than density and Poisson's ratio. With the increase of temperature, the first-order natural frequency of the double-panel partition moves to the low-frequency region. The first mode frequency and mode shape may not be observed when the temperature gradient gets greater, but the change of the

temperature gradient does not change the order of mode sequences and mode shapes.

- (2) The first trough of the sound transmission loss curve is determined by the first-order vibration mode of the panels. Under the temperature gradient of 0°C, 1°C, and 2°C, the first trough of the vertically incident sound transmission loss is 123 Hz, 99 Hz, and 64 Hz, respectively, which are consistent with the first mode frequencies. In the high-frequency region, the temperature gradient has little effect on the sound transmission loss under the vertical incidence.
- (3) When the size of the panel increases, the number of peaks and troughs on the curve decreases gradually and the curve becomes smoother. The small-size structure has more mode density than the large-size structure under the simply supported condition. In the middle- and high-frequency areas, the vertically incident sound transmission loss curve of the infinite simply supported double-panel partition provides an upper limit reference for the acoustic transmission loss of finite ones.
- (4) When the thickness ratio approaches 1.9 under the temperature gradient fixed at 2°C, the average sound transmission loss reaches the maximum value. It is shown that the thickness of the incident panel should be larger than that of the radiant panel to get greater average sound transmission loss.

Data Availability

The data used to support the findings of this study are available from the corresponding author upon request.

Conflicts of Interest

The authors declare no conflicts of interest.

Acknowledgments

The authors would like to thank the "13th Five-Year Plan" National Key R&D Plan of China (2016YFB1200500) and Major Strategic Projects of Chinese Academy of Engineering (2018-ZD-16) for their support.

References

- [1] Z. M. Wang and Z. X. Jiang, "Impedance analysis method for sound insulation of double panels," *Journal of Tongji University*, vol. 39, no. 9, pp. 1383–1386, 2011.
- [2] R. Zhao, K. P. Yu, and N. G. Cui, "Vibration response analysis of a composite sandwich plate under a time-varying thermal environment," *Journal of Vibration Engineering*, vol. 31, no. 2, pp. 151–157, 2018.
- [3] Y. D. Sha, L. Zhu, X. C. Luan et al., "Dynamic response of thin plates under thermal loadings with temperature gradient and acoustic loadings," *Journal of Vibration and Shock*, vol. 33, no. 18, pp. 102–109, 2014.
- [4] J.-M. Dhainaut, X. Guo, C. Mei, S. M. Spottswood, and H. F. Wolfe, "Nonlinear random response of panels in an

- elevated thermal-acoustic environment,” *Journal of Aircraft*, vol. 40, no. 4, pp. 683–691, 2003.
- [5] B. Behrens and M. Muller, “Technologies for thermal protection systems applied on re-usable launcher,” *Acta Astronautica*, vol. 55, no. 3–9, pp. 529–536, 2004.
- [6] D. Wu, Y. Wang, L. Shang, H. Wang, and Y. Pu, “Experimental and computational investigations of thermal modal parameters for a plate-structure under 1200°C high temperature environment,” *Measurement*, vol. 94, no. 12, pp. 80–91, 2016.
- [7] Y. Bai, K. Yu, R. Zhao, and H. Zhou, “Impact series shaker excitation approach for structural modal testing in thermal environments,” *Experimental Techniques*, vol. 42, no. 4, pp. 429–438, 2018.
- [8] Y. F. Zhou, L. L. He, X. Zhang et al., “Thermal modal analysis of typical thermo-defend panel structure,” *Chinese Journal of Applied Mechanics*, vol. 34, no. 1, pp. 43–49, 2017.
- [9] W. D. Wilson, “Speed of sound in distilled water as a function of temperature and pressure,” *The Journal of the Acoustical Society of America*, vol. 31, no. 8, pp. 1067–1072, 1959.
- [10] C. M. Kenneth, *Recommended Values of Thermophysical Properties for Selected Commercial Alloys*, Woodhead Publishing Limited, Cambridge, UK, 2002.
- [11] M. W. Kehoe and C. D. Vivian, *Correlation of Analytical and Experimental Hot Structure Vibration Results*, pp. 1–21, National Aeronautics and Space Administration, Washington, DC, USA, 1993.
- [12] Q. Geng, H. Li, and Y. Li, “Dynamic and acoustic response of a clamped rectangular plate in thermal environments: experiment and numerical simulation,” *The Journal of the Acoustical Society of America*, vol. 135, no. 5, pp. 2674–2682, 2014.
- [13] J. L. Maulbetsch, “Thermal stresses in plates,” *Applied Mechanics*, vol. 57, no. 2, pp. 141–146, 1935.
- [14] S. Brischetto and E. Carrera, “Thermomechanical effect in vibration analysis of one-layered and two-layered plates,” *International Journal of Applied Mechanics*, vol. 03, no. 1, pp. 161–185, 2011.
- [15] Y. C. Das and D. R. Navaratna, “Thermal bending of rectangular plate,” *Journal of the Aerospace Sciences*, vol. 29, no. 11, pp. 1400–1402, 1962.
- [16] Y. Liu and Y. Li, “Vibration and acoustic response of rectangular sandwich plate under thermal environment,” *Shock and Vibration*, vol. 20, no. 5, pp. 1011–1030, 2013.
- [17] T. R. Tauchert, “Thermally induced flexure, buckling, and vibration of plates,” *Applied Mechanics Reviews*, vol. 44, no. 8, pp. 347–360, 1991.
- [18] E. A. Thornatton, J. D. Kolenski, and R. P. Marino, “Finite element study of plate buckling induced by spatial temperature gradients,” in *Proceedings of the 34th Structures, Structural Dynamics and Materials Conference*, vol. 1, pp. 2313–2326, La Jolla, CA, USA, 1993.
- [19] N. Ganesan and M. S. Dhotarad, “Hybrid method for analysis of thermally stressed plates,” *Journal of Sound and Vibration*, vol. 94, no. 2, pp. 313–316, 1984.
- [20] Q. Geng and Y. M. Li, “Analysis of dynamic and acoustic radiation characters for a flat plate under thermal environments,” *International Journal of Applied Mechanics*, vol. 4, no. 3, Article ID 1250028, 2012.
- [21] F. X. Xin, J. Q. Gong, S. W. Ren, L. X. Huang, and T. J. Lu, “Thermoacoustic response of a simply supported isotropic rectangular plate in graded thermal environments,” *Applied Mathematical Modelling*, vol. 44, no. 4, pp. 456–469, 2017.
- [22] P. Jeyaraj, C. Padmanabhan, and N. Ganesan, “Vibration and acoustic response of an isotropic plate in a thermal environment,” *Journal of Vibration and Acoustics*, vol. 130, no. 5, Article ID 051005, 2008.
- [23] P. Jeyaraj, C. Padmanabhan, and N. Ganesan, “Vibration and acoustic response of a composite plate with inherent material damping in a thermal environment,” *Journal of Sound and Vibration*, vol. 320, no. 1-2, pp. 322–338, 2009.
- [24] P. Jeyaraj, C. Padmanabhan, and N. Ganesan, “Vibro-acoustic behavior of a multilayered viscoelastic sandwich plate under a thermal environment,” *Journal of Sandwich Structures & Materials*, vol. 13, no. 5, pp. 509–537, 2011.
- [25] K. Zhou, J. Su, and H. Hua, “Closed form solutions for vibration and sound radiation of orthotropic plates under thermal environment,” *International Journal of Structural Stability and Dynamics*, vol. 18, no. 7, Article ID 1850098, 2018.
- [26] P. M. Morse and K. U. Ingard, *Theoretical Acoustics*, Princeton University Press, Princeton, NJ, USA, 1987.
- [27] J. Wang, T. J. Lu, J. Woodhouse et al., “Sound transmission through lightweight double-leaf partitions: theoretical modeling,” *Journal of Sound and Vibration*, vol. 286, no. 4-5, pp. 817–847, 2005.
- [28] J.-P. Marage, *Sonars and Underwater Acoustics*, John Wiley & Sons, Hoboken, NJ, USA, 2010.
- [29] B. E. Gatewood, *Thermal Stresses*, McGraw-Hill, New York, NY, USA, 1957.
- [30] G. Lin, H. G. Guo, and Y. T. Zhao, *Aluminum Alloy Application Manual*, Mechanical Industry Press, Beijing, China, 2006.
- [31] F. X. Xin, T. J. Lu, and C. Q. Chen, “Vibroacoustic behavior of clamp mounted double-panel partition with enclosure air cavity,” *The Journal of the Acoustical Society of America*, vol. 124, no. 6, pp. 3604–3612, 2008.
- [32] M. Yairi, K. Sakagami, E. Sakagami, M. Morimoto, A. Minemura, and K. Andow, “Sound radiation from a double-leaf elastic plate with a point force excitation: effect of an interior panel on the structure-borne sound radiation,” *Applied Acoustics*, vol. 63, no. 7, pp. 737–757, 2002.